*Challenging Glass 7*
*Conference on Architectural and Structural Applications of Glass*
*Belis, Bos & Louter (Eds.), Ghent University, September 2020.*

*ISBN 978-94-6366-296-3, https://doi.org/10.7480/cgc.7.5051*

# Ultra Thin Composite Panel – An Exploratory Study on the Durability and Stiffness of a Composite Panel of Thin Glass and 3D printed Recycled PET

Charbel Miled Nohra Saleh [a, b] Christian Louter [a, c], Michela Turrin [a]
[a] *Delft University of Technology, Netherlands, c.m.n.saleh@hotmail.com*
[b] *Octatube Engineering B.V., Netherlands*
[c] *Technische Universität Dresden, Germany*

This paper investigates the stiffness and the durability of a composite panel that consists of thin glass as outer layers and a 3D printed core element from recycled PET. Thin alumino-silicate glass, mostly used for displays in computers, tablets and smartphones, is known for its flexibility, durability and high bending strength. However, for building applications, the high flexibility of thin glass may cause serviceability issues. Therefore, to stiffen thin glass, a composite concept of thin glass with a 3D printed core is developed. The core element of this panel consists of 3D printed recycled PET. The use of recycled PET has been taken into account, due to the increase of plastic waste for the next 30 years. A combination of both materials allows for a much stiffer composite panel and reduction in weight of 71,9 % compared to a normal double glazed window panel. This paper presents an overview of the durability of the composite panel. The durability aspects for this exploratory study are UV radiation, elevated temperature and fire. The UV radiation tests showed that the applied acrylic adhesive ensures for a good adhesion, which allows reaching high load bearing capacity. Also, these tests showed that recycled PET changes into a yellowish color and becomes more brittle. The temperature tests showed that at an elevated temperature of 80 ºC, recycled PET loses its stiffness and strength and cannot sufficiently take up forces when loaded. The fire experiments showed that the recycled PET core melted fully during the fire exposition

**Keywords:** Thin glass, Recycled PET, 3D printing, UV radiation, Elevated temperature, Fire, Honeycomb pattern, Truss pattern.

## 1. Introduction

Thin glass is seen as one of the upcoming material for the building environment, due to its flexibility, transparency, small thickness and associated low weight. One of the main challenges of thin glass is the lack of stiffness. It will be difficult for such a thin material to be stable enough under a load such as snow load and/or wind load. In combination with other materials, a stiff composite can be designed for different building components.

Plastic has developed into an essential material part of the society and also in the built environment. A research has shown that in the coming 30 years, the production of plastic will increase with 500%, also raising the risk of increasing the waste of plastic (Kreiger, Mulder, Glover, & Pearce, 2014). Introducing recycled PET into building components may help reducing the negative effect of plastic waste. In this light, challenging aspects of PET for applications in building construction are, amongst others: its low resistance against UV radiation and its sensitivity to temperature which may cause a degradation of its strength and stiffness.

Some studies have already been performed on the use of thin glass as a building component (Neeskens, 2018; Silveira, 2016). However, these studies did not yet investigate the durability of thin glass in combination with a 3D printed core of recycled PET. An MSc study was therefore made to determine the durability of the combination of thin glass panels with 3D printed recycled PET cores. The panels are tested on three durability aspects: UV radiation, elevated temperatures and fire. The research aimed at increasing the current knowledge on the structural behavior under these circumstances.

## 2. Background information

### *2.1. Thin glass*

The use of thin glass in the built environment is an innovative idea allowing several benefits. This is due to its small thickness (≤ 2mm), lightweight, flexibility (curved shapes), durability and bending strength and potential reduction of raw material usage in comparison with regular glass. It has also the potential to reduce the dimensioning of the supporting structure of a building due to its low selfweight. However, the lack of stiffness and instability of the thin glass may cause serviceability issues such as too much deformation. As a solution, the combination with other materials can lead to manufacturing a stiff panel that can be used as a building component.

In this study, thin alumino-silicate glass is used. Compared with regular soda-lime silica glass, alumino-silicate glass has a lower percentage mass of silica sand ($SiO_2$) and higher alumina ($Al_2O_3$) content. The alumino-silicate glass used in this study is Falcon (AGC) with a thickness of 1.1 mm and has been chemically strengthened. In table 1 the material properties of the Falcon glass are shown.

Table 1: Properties of Falcon glass from AGC (AGC, 2017, p. 2).

| | AGC Falcon™ glass (Alumino-silicate glass) |
|---|---|
| Density | 2480 kg/m$^3$ |
| Young's Modulus | 73.000 MPa |
| Poisson ratio | 0,22 |
| Shear Modulus | 30.000 MPa |
| Softening point | 665 ºC |
| Coefficient of Thermal Expansion | 9,10 * 10$^{-6}$ K$^{-1}$ |
| Glass Temperature (Tg) | 575 ºC |

## *2.2. Recycled PET*

PET (abbreviation for polyethylene terephthalate)is a semi-crystalline polymer of the group polyesters and belongs to the group thermoplastic (López-Fonseca et al., 2011; CES Edupack, 2017; Al- Sabagh et al. , 2016). Among plastics, PET outstands in the food packaging, bottles and building industry due to its high tensile and impact strength, chemical resistant, transparency, clarity processability, colour ability and thermal stability. Also, PET may have high molecular weight (MW), which provides stiffness, toughness, creep resistance and a certain degree of flexibility. However, it should be noted this does not apply to PET for all applications. For example, textile fiber-grade PET has a lower molecular weight than bottle grade PET (Al-Sabagh et al., 2016; Awaja & Pavel, 2005; Park & Kim, 2014). Another characteristic of PET material is it fair resistance against UV radiation. PET ages when it is exposed to UV (light) and oxygen, changing its properties such as strength, stiffness and toughness. Also, PET is subject to changes color (yellowish), loss of transparency, loss of gloss and becomes brittle (CESEduPack, 2017; PTI, 2015). This is relevant also when considering applications in the built environment. One of the important issues for facades in the built environment is are the high temperature at summer. Depending on local climate, in summer temperatures on facades can easily reach 40-60 ºC. When the temperature increases, the polymer loses its strength and rigidity. The main transition happen at the melting point temperature ($T_m$), at which the crystalline regions breaks of the polymer, due to chain rotation (Al- Sabagh et al. , 2016).

In 2017, the worldwide plastic consumption was 19.1 million tons and is expected to increase with 5,2 % yearly (Park & Kim, 2014). From this plastic consumption, only 14% of plastic packaging and bottles is collected (EllenMacArthurFoundation, 2014). From this only 55 % consists of PET bottles (in 2012) and is recycled, but this differs from each country. PET can be recycled based on two different methods: mechanical recycling and chemical recycling; contributing to the reduction of the waste of PET (Awaja & Pavel, 2005).

Among possible uses, the PET collected for recycling can be manufactured into filament or pellets for 3D printing. As an example, this may regard PET bottles collected by recycling suppliers or waste pickers; then cleaned to remove all the dirt and dried; finally shredded into the desired flakes, as mentioned in table 6. The flakes have mostly the desired size of 6mm. These are filtered and the one that are larger than the desired dimension, are being collected and placed in the shredder again. To produce filament, the filtered flakes will be processed further in the extrusion machine. Here the flakes are being melted above the glass transition temperature ($T_g$), where the flakes melt and extruded. The extruded filament is being rolled onto a spool where it can be packaged for the use as filament for 3D printing. To guarantee a good quality of recycled filament, some tests are made to see if it meets the requirements. After these stages of processing, the filament is transported to be sold for the consumer (RefabDar, 2016; Reflow, n.d.)

The production of recycled PET filament from recycled PET bottles has shown that the filament has a constant density, a uniform diameter and transparent (Baechler et al., 2013). As an example, usually the Refil recycled filament is not 100% fully recycled, due to the degradation of the mechanical properties; and about 10 percent might be virgin PET material for improving the mechanical properties of the filament (Refil, n.d.). An evaluation of different tests of the recycled PET filament has been made by Horne (2015), mentioning the quality of printing with the recycled filament is very much alike as the normal (virgin) PET filament. Nevertheless, the physical properties differ slightly from each other, due to the sensitivity to temperature and printing speed. Looking for example at some technical properties provided by the company Refil (Refil, n.d.): The density of recycled PET filament ranges between 1350 and 1380 kg/m$^2$ and the tensile strength is 50 MPa (Refil, n.d.). Compared with the virgin PET filament, this has a lower tensile strength. This can be due to the recycling process, in which the properties of recycled PET decrease. If the filament was 100% recycled, the strength would be expected to be much lower. It is also worth noting not all the mechanical properties are fully known, due to current lack of research of recycled PET filament.

### *2.3. 3D Printing (FDM)*

The ASTM (American Society for Testing and Materials) defines additive manufacturing (AM) as “the process of joining materials to make objects from 3D model data, usually layer upon layer, as opposed to subtractive manufacturing methodologies”. AM has been growing rapidly and becoming one of the important production processes, where a 3D model can be manufactured to a final product. One of the advantages of using AM is the fabrication of complex geometries in one piece, eventually allowing rapid installation due to reduced and simplified connections.

In recent years, the 3D printing technique Fused Deposition Modeling (FDM), which is a form of AM, is increasingly used in product development processes, not only for the aerospace and automotive manufacturing, but also for the construction in the building industry (Lim et al., 2012). In FDM, a rolled string, filament, is guided to a reel into a heated nozzle. Here the filament melts and can be extruded in a particular and predetermined way. This nozzle can move, in most common 3D printers in two axis, the xy axis. The movement decided in advance by a 3D printed software. The material that is extruded and deposited is instantly cooled down and solidified. This will function as the base for the next layer. This is repeated for every layer till the object is fully printed.

Like each production method, also FDM offers both opportunities and limitations.. Opportunities are as follow (Delgado et al., 2018) :

- Possible production of complex geometries;
- Possible production of customized products, without extra costs for the manufacturing of non-standardized pieces (figure 1a);
- Possible lower costs, compared with methods requiring e.g. molds and tools needed;
- Possible reduced lead time and quick start production;
- Possible reduction of waste during production (uses only the material that is needed for an object);
- Small batch production**.**

Despite the advantages, as production method FDM has also some limitations, resulting in possible drawbacks compared with conventional manufacturing. One limitation is the higher costs when it comes to production of a large production of batches. In figure 1b, a schematic diagram is given with the costs of batches against the number of components. This shows that up to a certain amount of batches (turning point between 1000 and 10.000 batches) it is more cost effective to use the additive manufacturing, in comparison with injection moulding (Lim et al., 2012).

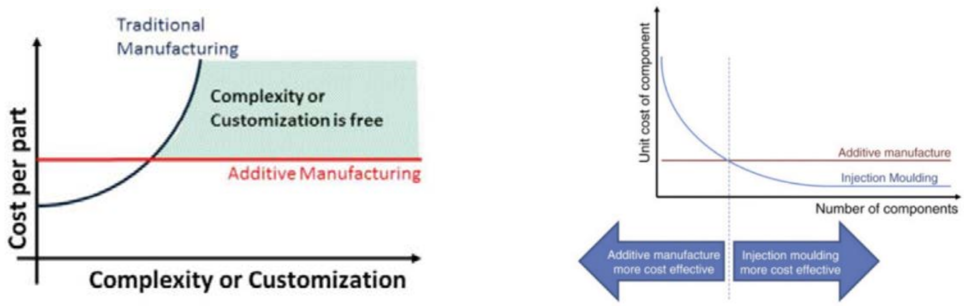


a) b)

Fig. 1 a) Comparison of AM and Traditional manufacturing. Complexity and Customization becomes free with AM (Conner et al., 2014), b) Cost diagram for AM and CM (Lim et al., 2012).

## 3. Studying the structural properties of 3D printed PET and Recycled PET

Since there is a lack of research on the use of recycled PET as a filament for 3D printing, investigating the mechanical properties and structural behavior of recycled PET and comparing it with PET is necessary. Aiming at this, tests have been run and the results are presented in this paper.

### *3.1. Characterization of 3D printed recycled PET and PET (unaffected)*

Tensile properties of the recycled PET- and PET 3D printed specimens (unaffected) and 3D printed specimens (UV exposed) were tested using a ZwickRoell Z010 tensile testing machine. To be able to do the tensile testing after the material is 3D printed, specimens were 3D printed in a specified shape (based on NEN-ISO 527-1 standard). Those are so called dumbbell/dog-bone specimens. The specific dimensions of the specimens are shown in figure 2a . The specimens were loaded in tension a rate of 5 mm/min. Five specimens were 3D printed for each material. These can be seen in the 2b and 2c.

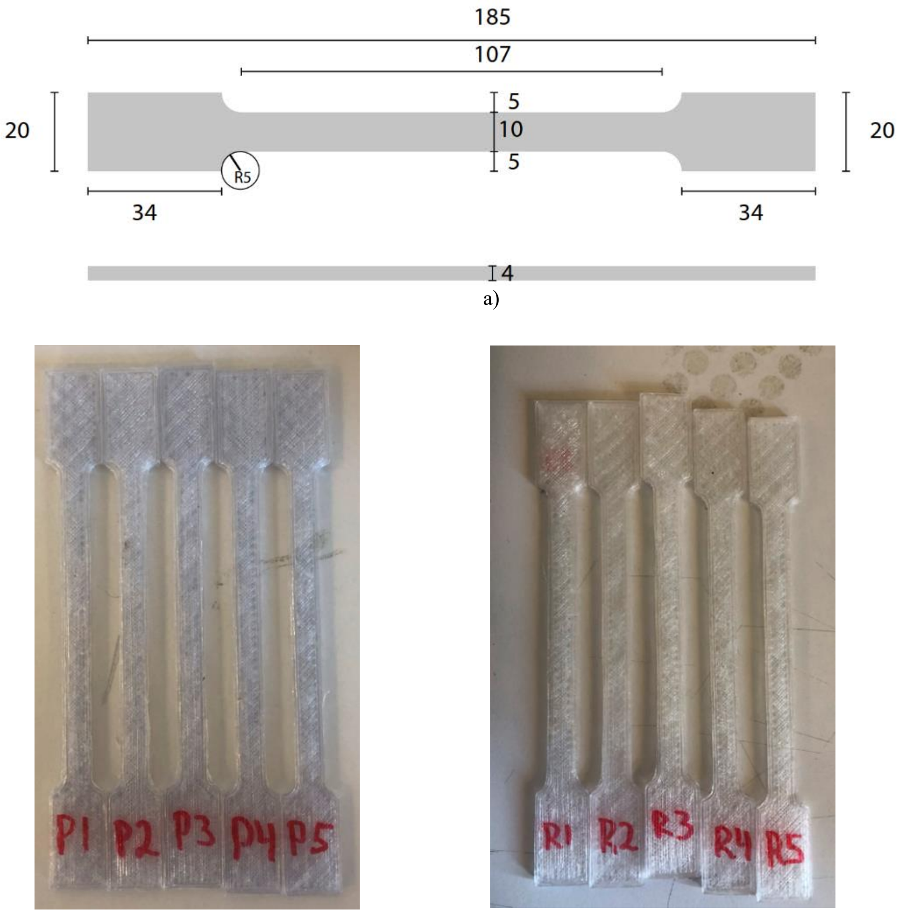


Fig. 2a) dimensions dumbbell specimens based on NEN-ISO 527-1 Standard, b) 3D printed PET specimens, c) 3D printed Recycled PET specimens.

### *3.2. Characterization of 3D printed recycled PET and PET (UV aged)*

An UV accelerated weathering tester is used to accelerate the UV ageing of the 3D printed dumbbell specimens of PET and RPET. The UV test machine (model HST-UV-A) is a machine that provides the heat of the sun and UV radiation. Also, it uses a UV lamp of 300 Watt. This allows for the a faster UV-radiation in a short time and observing the anti-yellowing degree of a sample after a period of time. The internal wall of the machine consists out of mirror finished stainless steel. This allows for the light to reflect on to the walls and to the specimens (environmental test-chamber, 2018).

The settings of the of the thermostat are set to PV 34.3 and SV 50. The specimens are placed for two weeks (336 hours) into the UV machine before being tested (ZwickRoell Z010) to see what kind of effects UV ageing has on PET and RPET and its mechanical properties (figure 3).

Fig. 3 Accelerated UV source with 3D printed specimens.

### *3.3. Mechanical properties of 3D printed recycled PET and PET (unaffected and UV aged)*

The results of the tensile tests of the specimens with Zwick Roell Z010 can be seen in table 4. For the tested specimens, these have shown that the Young's modulus of recycled PET Filament is 25 % lower than PET filament. Also, the maximum tensile strength of recycled PET resulted 30 % lower than normal PET filament. For both cases, this is expected to be due to the process of recycling PET, as mechanical recycling allows for PET to degrade during the recycling process.

The results (table 2) allowed considerations also on the effect of 3D printing on the mechanical properties of PET and RPET. For the tested specimens, compared to the PET filament, the Young's modulus of 3D printed PET decreases with a factor 2.70 and the maximum strength (tensile strength) with a factor 1.56. Also, the recycled PET decreases in Young's modulus and strength. This is a factor of 2.27 and 1.16 respectively. It can be expected the reduction arises due to the crystallization of the polymer, the process from melting to solidification. After the extrusion of the melted filament, one side of the surface can cool while the other part can still be hot. This can generate higher internal stresses in the material, which grants for lowering the strength of the material (Frankland, 2013). Also, by comparing the 3D printed PET and RPET with each other, both mechanical properties do not differ respectively so much from each other. The 3D printed recycled PET is approximate + 10 % lower than the normal 3D printed PET.

With regard to the UV aged specimens, the results show that the PET and RPET become stiffer after UV radiation, but have a lower strain percentage. This means that the material can assume a higher force, but fails relatively faster due to the lower strain percentage. This shows also that both materials become more brittle and showed a brittle failure. Also, their maximum strength decreases compared with the unaffected specimens.

It can be observed the strength of the RPET and PET depend on the exposure UV radiation. This implies that the UV-exposed specimens fail at a lower stress. Another important aspect is that RPET and PET change color after due to UV exposure. The color change effect is at the RPET higher than PET. In figure 4 the color change is shown of the Recycled PET and PET.

Table 2: Results of the tensile test of the 3D printed specimens of PET and Recycled PET (unaffected and UV aged).

| Specimens | Young's Modulus [MPa] | Tensile strength [MPa] |
|---|---|---|
| PET 3D printed | 1093.4 | 33.5 |
| Recycled PET 3d printed | 980.3 | 31.3 |
| PET 3D Printed UV exposed | 1482.0 | 27.3 |
| Recycled PET 3d printed UV exposed | 1120.3 | 28.5 |


(a) (b)

Fig. 4a) UV ageing of 3D printed PET specimens after two weeks, b) UV ageing of 3D printed recycled PET specimens after two weeks

## 4. Structural behavior and FEM analysis

After the tests presented in previous section regarding specimens, the research considered the scale of the panels. For panels with different patterns, Finite element analyses were performed to investigate their structural behavior. Also, some typologies have been physically produced and tested. To be able to see how the panel would behave practically, prototype composite panels were modelled and built with dimensions of 250 x 150 x 12.2 mm.

### *4.1. Core topologies*

The first pattern studied here, a homogeneous core, is a fully closed pattern and has a homogeneous support of the top and bottoms skins (figure 5a). This core has a dimensioning of 250 x 150 x 10 mm and has a weight of 506.25 grams. This topology is numerically analyzed in the software DIANA FEA with a structural nonlinear analysis. This type of core was not built due to the high printing time and relatively high weight of the core.

The second pattern chosen for this research is the honeycomb pattern (figure 5b). Based on the study of Vitalis (2017), the honeycomb pattern has a relatively high stiffness and low density. Earlier studies were also made with a honeycomb pattern, but smaller cells and made from aramid (Louter et.al., 2018). The honeycomb pattern belongs to the so called ‘structured’ (non-homogeneous) support for the outer layers (Thomsen, 2009). Also, this pattern is only in the direction of the height/thickness. This allows for a better optical quality, lightweight and the transfer of shear stresses. The prototype honeycomb pattern has the same length, width and thickness as the previous pattern. The thickness of each honeycomb cell is set at 1mm. By combining the cells to each other ensures for doubling the thickness of each wall surface to 2mm. One of the aspects of choosing this thickness, is the use as less as possible wall thickness to allow for a lower weight and better optical effect.

The last pattern is the truss pattern which was studied by Akilo (2018) (figure 5c). He showed that the truss pattern has a relatively low density and high strength. This pattern differs from the other patterns, due to its the punctual supports of the skins. Just like the honeycomb pattern, the truss pattern belongs to the ‘structured’ (non-homogeneous) supports of the skins.

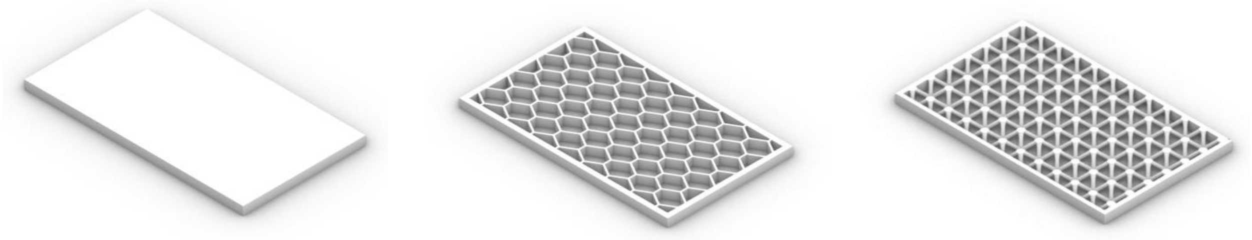

(a) (b) (c)

Fig. 5a) homogenous core , b) honeycomb core, c) truss core.

### *4.2. Numerical analysis (structural behavior)*

The numerical analysis are performed in the DIANA FEA software and are based on a 3 point bending test. The input and geometry dimensions are based on the previous properties of the materials. The parameters of the thin glass are based on the technical data of the glass from the company AGC. The Recycled PET properties are based on the technical data from Refill and from the tests that was presented in section 3.3.

After analyzing the structural behavior of the different typologies in DIANA FEA, the three different typologies showed a dissimilar performance (figure 6). Comparing the deflection of the panels with each other (table 3), the panel with the homogeneous core has the lowest deflection and the one with the truss core has the highest deflection. The deformation of the honeycomb is higher with a factor 3.13 than the homogeneous core, but the weight of the honeycomb core is 4.3 times smaller. The Truss has almost the same weight as the honeycomb core, but showed a deformation of a factor 2 higher than the honeycomb and 6 times higher than the homogeneous core. The similarity of the three panels, is that highest the deflection is in the middle of the panel. The same comparison is done for the shear stresses. Noticeable is that the highest shear stresses occur at the truss pattern. These are, compared with the homogeneous- and honeycomb core, 4.0 and 3.0 times higher respectively. The highest shear stresses occur on the edges of the panel, where the supports are. The areas where the highest shear stresses appear will ensure where the panel could fail.

Table 3: Output FEM analysis with a load of 40 N.

| Composite panel | Maximum deflection [mm] | Maximum Shear stress [N/mm$^2$] |
|---|---|---|
| Homogenous core | 0.0197 | $\pm$ 0.0450 |
| Honeycomb core | 0.0356 | $\pm$ 0.0735 |
| Truss core | 0.1233 | $\pm$ 0.1821 |

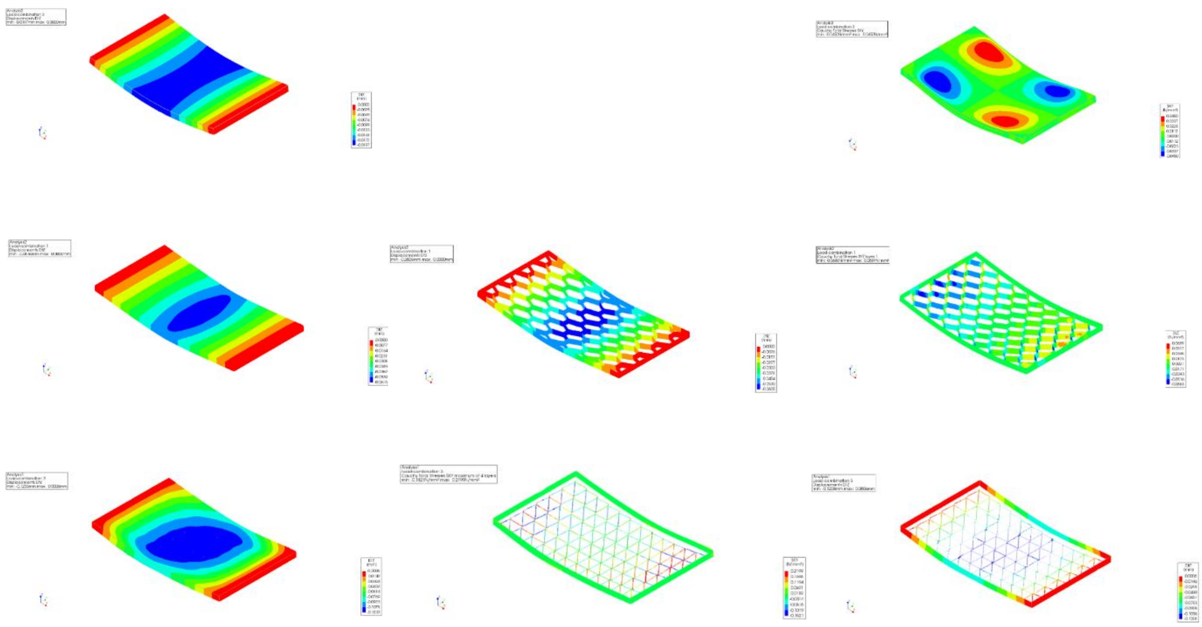

Fig. 6 Overview of the output of the FEM analysis (deflection panel(left), deflection core(middle) and shear stresses in the core(right)) of the three composite panels with the following cores: homogenous, honeycomb and truss.

### *4.3. Numerical analysis (Heat flow)*

A heat flow analysis was performed in DIANA FEA.. This analysis was performed to determine the heat flow through the panel during a fire. This was done for the composite panel with three different cores.
The geometry of the panel and supports is shown in figure 7a. Above the thin glass panel (bottom layer), the surface on the inside, the temperature is almost the same as the outer surface. This is expected to be due to the low thermal resistance of the glass panel. The thin dimensioning allows for high thermal transmittance through the panel. This ensures that the core of RPET would start melting after 30 seconds and the panel will start decreasing in stiffness. The melting will take place in layer by layer for all the three patterns. The honeycomb and truss core are expected to melt faster due to the openness of the pattern, which allows the heat transmit for bottom and side. The melting for both patterns also takes place layer by layer (figure 7 b,c,d).

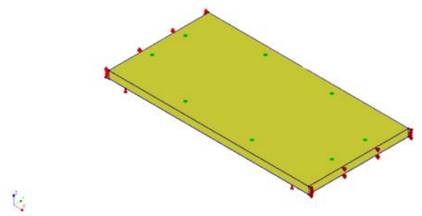

(a)

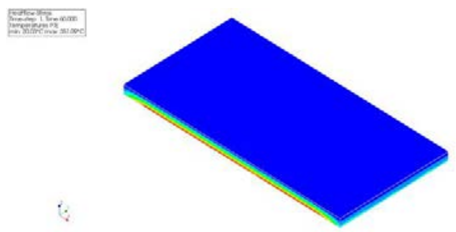

(b)

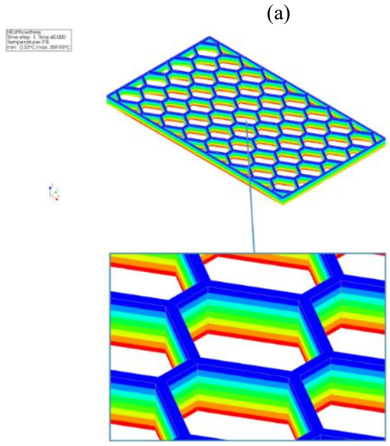

(c)

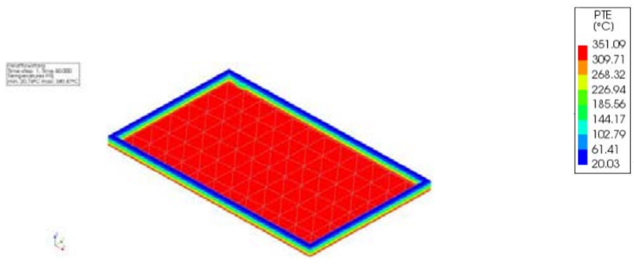


(d)

Fig. 7a) setup panel in Diana FEA , b) Output heat flow composite panel with homogenous core, c) Output heat flow composite panel with honeycomb core, d) Output heat flow composite panel truss core.

The thin glass as face skins of a sandwich panel allows for a high transmittance of heat through the glass, due to its relatively low thickness. This high transmittance allows for the recycled PET core to melt. The glass transition temperature ($T_g$) of recycled PET is 75 $^{O}$C, at which the stiffness of the core material (recycled PET) will start to decrease significantly . Afterwards, the temperature will increase to a temperature of 349 $^{O}$C after 1 min and the core material will melt.. For recycled PET, this melting starts at its melting temperature of 195 $^{O}$C.
Comparing the three topologies, we can see that the sandwich panels with the honeycomb- and truss core melt relatively faster than the homogeneous core. This is due to the open cells of both patterns and the relatively less use of material.

## 5. Physical tests and results

In this section the assembling of the panels and the setup of the experiments is elaborated. A total of 4 test series were performed. A 3-point bending test was done on panels that are unaffected, UV aged and one with elevated temperatures. Also, an experiment was done to see how the sandwich panel behaves during a fire (high temperatures).

### *5.1. Prototype*

The sandwich panels consists out of two outer face skins of alumino-silicate glass of 1.1 mm and a 3D printed recycled PET core of t=10 mm. The core is one of the most important part of the sandwich panel, because this part is where the highest shear stresses arise. The core panels are printed with a Leapfrog Creatr with a single extruder of 0.8 mm.
Once the core is printed, the adhesive is applied on the outer surface of the 3D printed core. The adhesive used for this research is the DELO photobond 4494. This adhesive is a transparent and UV- and light curing acrylate adhesive with a medium viscosity. It is a one-component altered modified urethane acrylate adhesive . This adhesive can be used for plastic on plastic, glass to plastic and glass to glass bonding.
When the adhesive is applied to the surface, the following step is to clean the thin glass surface, where it will be bonded. This is done by applying isopropanol on a tissue paper and then clean the glass in one direction. This allows for all the dust on the glass surface to be removed. Afterwards, the glass panel can be placed on the RPET core surface, which results in the prototype that can be seen in figure 8a & 8b.

(a) (b)

Fig. 8a) Test panel with thin glass and 3D printed honeycomb recycled PET core, b) Test panel with thin glass and 3D printed truss recycled PET core.

### *5.2. Bending test 1: Recycled PET core*

The first test was a 3 point bending test experiment. In this test, the panels are bended in the middle through a loading steel pin and will be supported on the edges with a steel supporting pin. The highest deformation of the sandwich panel and maximum bending moment occurs in the middle of the panel, where the load is applied (figure 9).

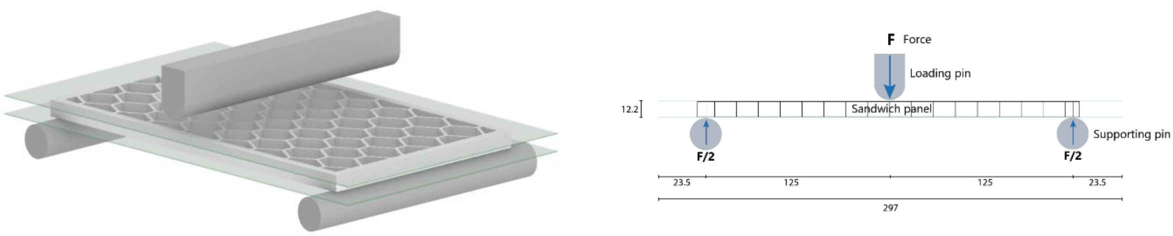


Fig. 9 Principle and setup for the 3 point bending test.

The 3 point bending test was performed with the Zwick Roell Z100 for the two different recycled PET core patterns. The Zwick Roell Z100 was chosen due to the dimension of panels and the setup equipment. The bending test was performed with a speed of 10mm/min and was set up to maximum deflection of 50mm. The results of those two pattern is shown in figure 10a and 10b. According to the results, both panels could deform up to 50 mm. This shows that the recycled PET core could deform significantly without failing. The first cracks occurred on the edges of both panels. The output of both experiments (in diagram 01) show the honeycomb core reached a higher bending force than truss pattern. The maximum force is respectively 227.51 N and 164.48 N. By comparing the results of both patterns, the honeycomb bending stiffness results higher with a factor 1.5. At a deformation of 47 mm the honeycomb core failed at the edge, were the first crack started. The truss pattern did not fail at a deformation of 50mm, when the experiment was stopped.

(a) (b)

Fig. 10a) Honeycomb recycled PET core at a deflection of 50 mm, b) Truss recycled PET core at a deflection of 50 mm.

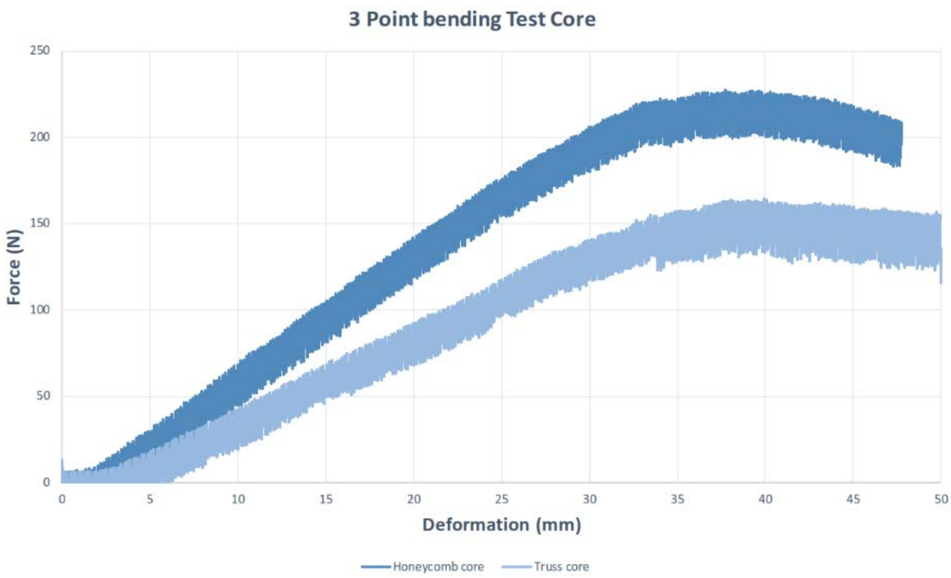


Diagram 01: Result 3 – point bending test core element.

### *5.3. Bending test 2: Composite panel of thin glass and recycled PET core*

The second test performed on the composite panels consisted of 1.1 mm of Falcon thin glass (as facing skins) and recycled PET core. The settings were the same as for the testing of the cores. Four unaffected panels were tested, two of each pattern. Those were deformed to a maximum displacement of 50 mm upon which the tests were stopped.

The results of the 3 PBT (diagram 2a,b,c) on the panels shows that three of the four panels have risen to their maximum force and afterwards decreased. The maximum force of composite panels with honeycomb core (HC 1 and HC 2) and truss core (Truss 1 and Truss 2) are respectively 724 N(HC_1), 763 N (HC_2), 609 N (Truss_1) and 821 N (Truss_2). The decreasing effect seems due to the detachment of the adhesive between the panel and the glass surfaces. The panel with the most adhesive surface (Truss 2) showed to behave structurally stiffer than all the three other panels before reaching its maximum strength, but decreased relatively more than the HC 2 panel. Afterwards, the force started increasing again till the first crack arises and decreased again.

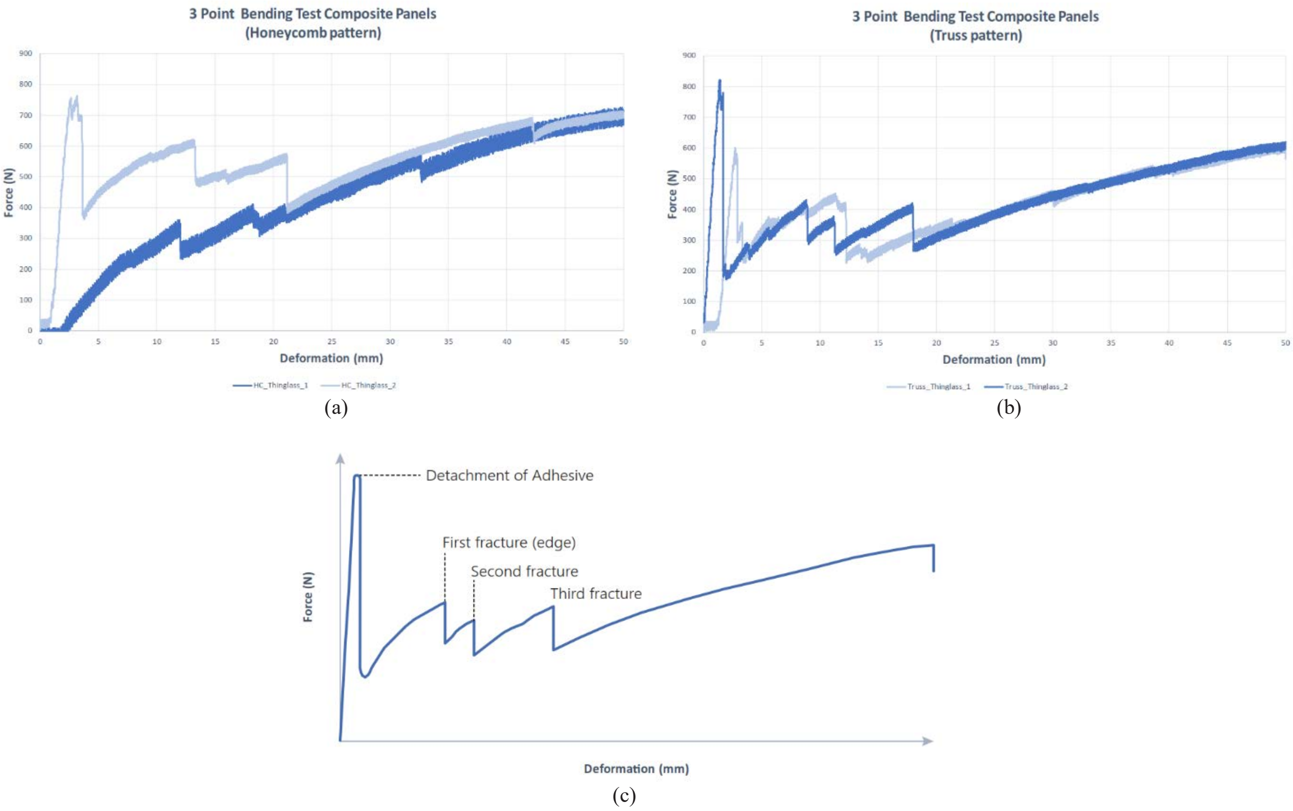


Diagram 2a) Result of 3 PBT unaffected composite panel with honeycomb pattern, b) Result of 3 PBT unaffected composite panel with truss pattern, c) structural behavior of the composite panel unaffected.

### *5.4. Bending test 3: Elevated temperature (summer conditions)*

The third experiment was an experiment where the composite panel is tested in 3-point bending in a climate chamber (figure 11). The aim of the test is to determine the structural behavior of the core and sandwich panel at elevated temperatures, e.g. in summer conditions. Based on the ETAG- 002 standards, surfaces of panels can reach op to a temperature of 80 degrees Celsius in the summer conditions.

Fig. 11 3-Point bending test setup for elevated temperatures.

The first experiments with elevated temperatures was performed on the recycled PET core of with the honeycomb and truss pattern. Both cores were placed in the oven for 5 min to be heated up and afterwards placed on the setup. The honeycomb- and truss core started to deform due to their own weight (figure 12a & b). Here, the core reached its glass transition temperature ($T_g$). A pre-load of 20 N was applied to the core. Even with this relatively low force, the core could not stand. Both panels had distortion due to own weight at a temperature of 80 ºC. In this experiment no cracks or failures were detected.

a

b

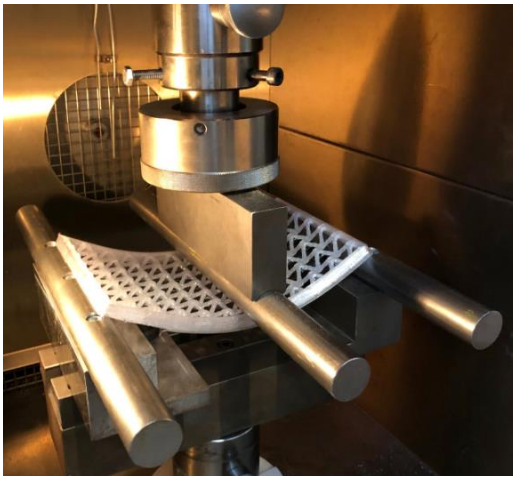

Fig. 12a) Recycled PET core with honeycomb pattern deflection without a force at 80 $^0$C, b) Recycled PET core with truss pattern deflection at 80 $^0$C.

The second experiment at elevated temperatures was performed with the sandwich panels. The panels were placed in the oven for 15 min to be preheated and then a force was applied onto the composite panels. Both panels were deformed to 50mm (figure 13a&b).

The results show that the truss pattern behaved stiffer than the honeycomb pattern and showed a more ductile behavior. Here, the truss reached its maximum yield strength and started drawing. The load-displacement diagram also showed some drops in forces. This is where the adhesive started detaching from the core and the top glass surface (diagram 3). The panel behaved first elastically and afterwards plastically. The yield force for this pattern is 496 N. The ultimate force reached for the truss pattern is 615 N for a deformation of 50mm.

In contrary, the composite panel with a honeycomb core behaved less stiff than the truss pattern. However, the panel behaved elastically till the maximum deformation of 50mm. At this deformation, the composite panel reached its maximum yield strength. Compared to the truss pattern, the yield force of the honeycomb panel is relatively 1.2 times

a

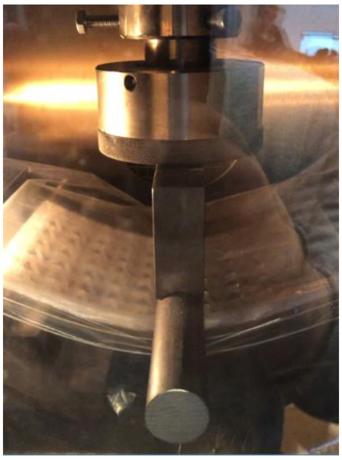

b

Fig. 13a) Composite panel (honeycomb core) with a deflection of 50mm at 80 $^0$C, b) Composite panel (truss core) with a deflection of 50mm at 80 $^0$C.

higher than the truss panel. Here the yield force is 592 N. This test, the panel with the honeycomb pattern, did not reach its ultimate force yet. Also, for this pattern no cracks occurred. But the distortion of the core pattern shown remarkable aspects as the core started to deform due to the shear stresses that occurred. A possible expectation would be that the panel with a honeycomb core would have reached higher forces, but the bending radius of the glass panel would have increased and fail.

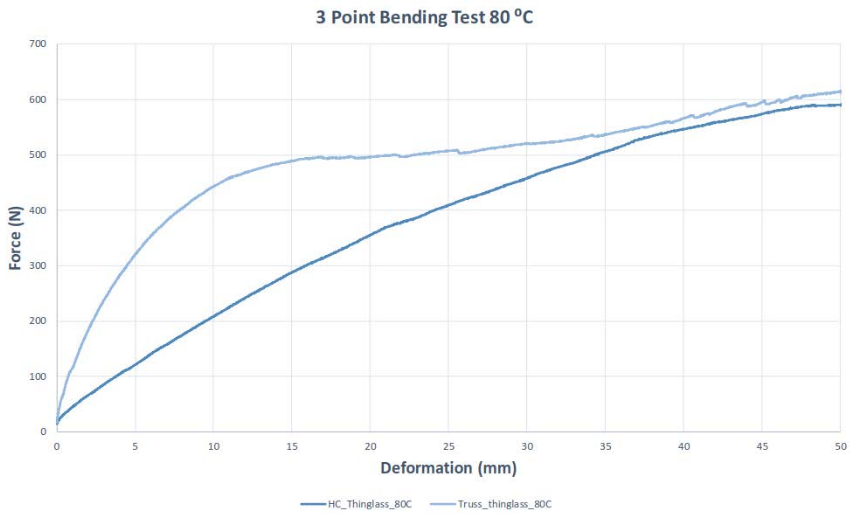


Diagram 3: Results of the 3 PBT at a temperature of 80 $^0$C.

### *5.5. Bending test 5: UV aged*

The fourth test was the UV aging of the composite panels. Here, the panels were exposed to UV (accelerated) for a period of time and tested. The UV source light is a point light which allows the intensity of radiation of UV to take place at one specific area of the panel. This test allows to see how the panels structurally behave after UV ageing. The composite panels were placed into the UV accelerated weathering test machine for two weeks (336 hours). Figure 14a shows the panels in the test machine. The panels were placed diagonally in the test-machine due to the dimensioning of the panels. The panels were turned around after 168 hours.
After 336 hours of UV radiation in the UV accelerated test machine, the panels showed that the core of the sandwich panels changed color. In comparison with the unaffected panel, the UV radiation allows for the recycled PET to change into a yellowish color (figure 14b&c).

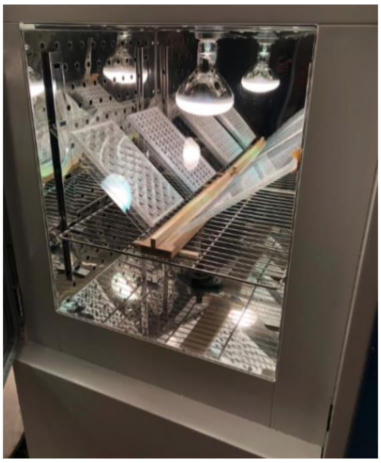

(a)

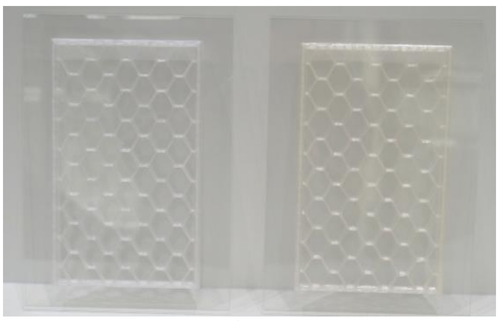

(b)

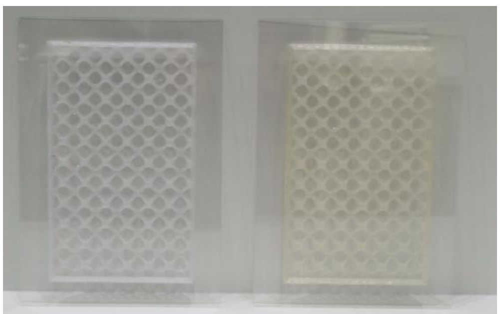

(c)

Fig. 14a) Composite panels setup in the UV accelerated test machine, b) composite panel with honeycomb pattern unaged(left) and 336 hours UV aged (right), c) composite panel with truss pattern unaged(left) and 336 hours UV aged (right).

To be able to see if the UV radiation also effects the stiffness of the panels, a 3 point bending test was performed with the Zwick Roell Z100. Looking at the results of the test, it is noticeable that the UV aged sandwich panels are stiffer than the unaffected panels. The first panel tested was the one with the honeycomb pattern. This panel reached a maximum force of 1709 N. This is 2.3 times higher than the unaffected panel with a honeycomb pattern. The second one was 1070 N (diagram 4a). The same also happened for the panel with truss core. Here, the maximum force is 1346 N and 1089 N (diagram 4b). The difference of reaching maximum forces is expected to be due to the amount of adhesive used for the bonding of the composite panels. The Delobond adhesive is expected to have cured further by the UV radiation, which allowed for a better bonding between the core and thin glass surface.

The honeycomb core element started cracking at edge and continued to crack where the highest shear stresses occurred (figure 15a). The composite panels with a honeycomb pattern failed during the bending test. The first one broke at a deflection of 50 mm and the other one at 26 mm. Both elements, thin glass and recycled PET core, broke. A reason for this failure is the detachment of the adhesive and the failure of the core element, which allows the panels to have a smaller bending radius, leading to higher stresses in between the layers and causing the failure. On the contrary, the UV aged panels with a truss core pattern did not fail. Here, only the core failed, but the glass skins did not break. The core material became more brittle and could not allow to take the high shear stresses which allowed for the breakage pattern in the core (figure 15a&b). The schematic structural behavior of the composite panels with different core patterns is shown in diagram 4c.

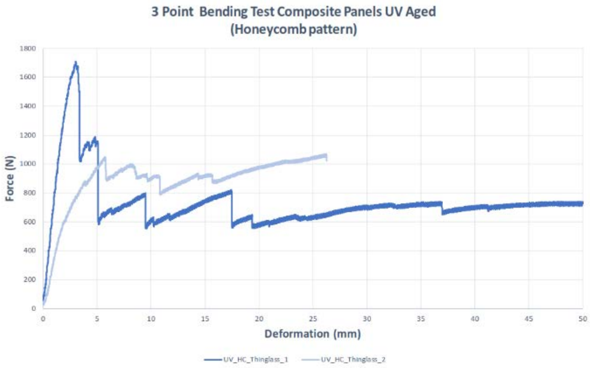


(a)

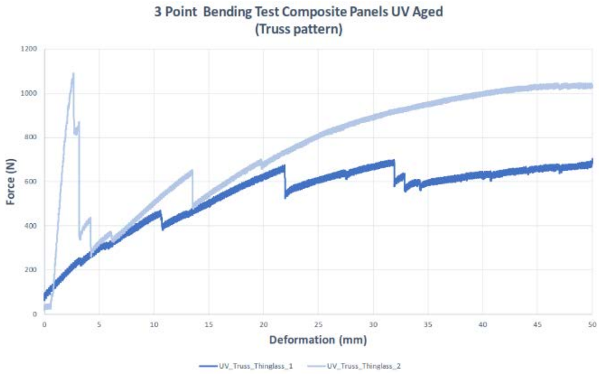


(b)

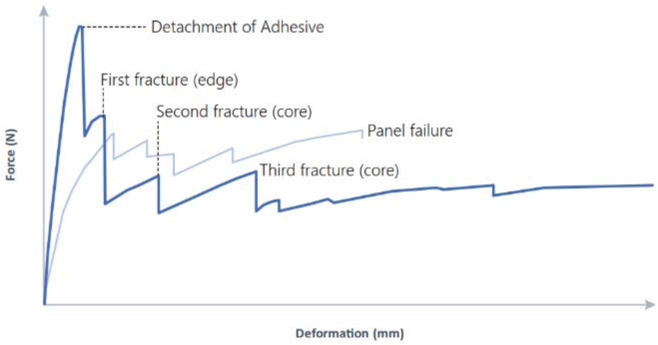


(c)

Diagram 4a) Result of 3 PBT of UV aged composite panels with a honeycomb core, b) Result of 3 PBT of UV aged composite panels with a truss core, c) structural behavior composite panels (UV aged).

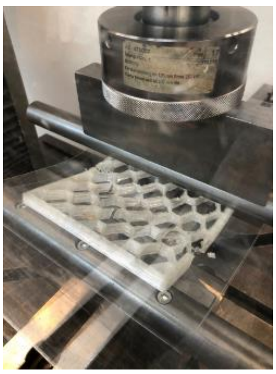

(a)

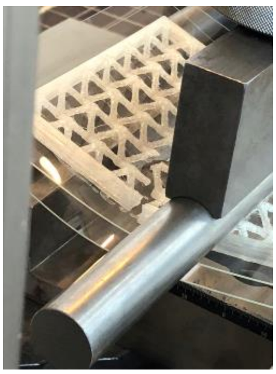

(b)

Fig. 15a) failure of honeycomb core element of the composite panel(highest shear stresses), b)failure of truss core element of the composite panel(highest shear stresses).

### *5.6. Bending test 4: Fire*

The fifth test was the test of the sandwich panel against fire. A set up was made to reach high temperatures (350 $^{O}$C-400 $^{O}$C) and the observations and the behavior of the panel. The fire test setup is made to be able to see how the sandwich panels structurally behave during a fire and what happens with both materials during the high temperatures. The setup consists of fire bricks and a fire source (gas burner) (figure 16a). Fire bricks are used since they hold up the heat inside. The panel is placed above the bricks with a load on top of it (figure 16b). The panel was heated up from the bottom side. The temperature of inside the setup and the panel was measured with an infrared thermometer.
First, the sandwich panel with a truss pattern was tested. The temperature started at 165 $^{O}$C and was heated up to a temperature of 350 $^{O}$C. At a temperature of 125.7 $^{O}$C at the inside of the setup, RPET core started becoming viscous and started melting. At a higher temperature, around 303 $^{O}$C, the RPET started changing color becoming yellowish and when the temperatures rises it becomes brownish (figure 16c). Also, at the high temperatures smoke started arising and a sweetish smell from the edges of the panel.
Secondly, the sandwich panel with honeycomb pattern was tested with a fire source from underneath it. The same steps as the one mentioned before, were made. The same principles occurred in this experiment. The bottom thin glass panel started heating up, where at a temperature of 175 $^{O}$C (measured with the infrared thermometer) the first layers of the core started melting (figure 16d). The bottom panel started deflecting on the edges and the molten core material started dripping out. The dripping out occurred also due to the force that was placed on top of the panel. The RPET core is partly burned and partly dripped out (figure 16e).

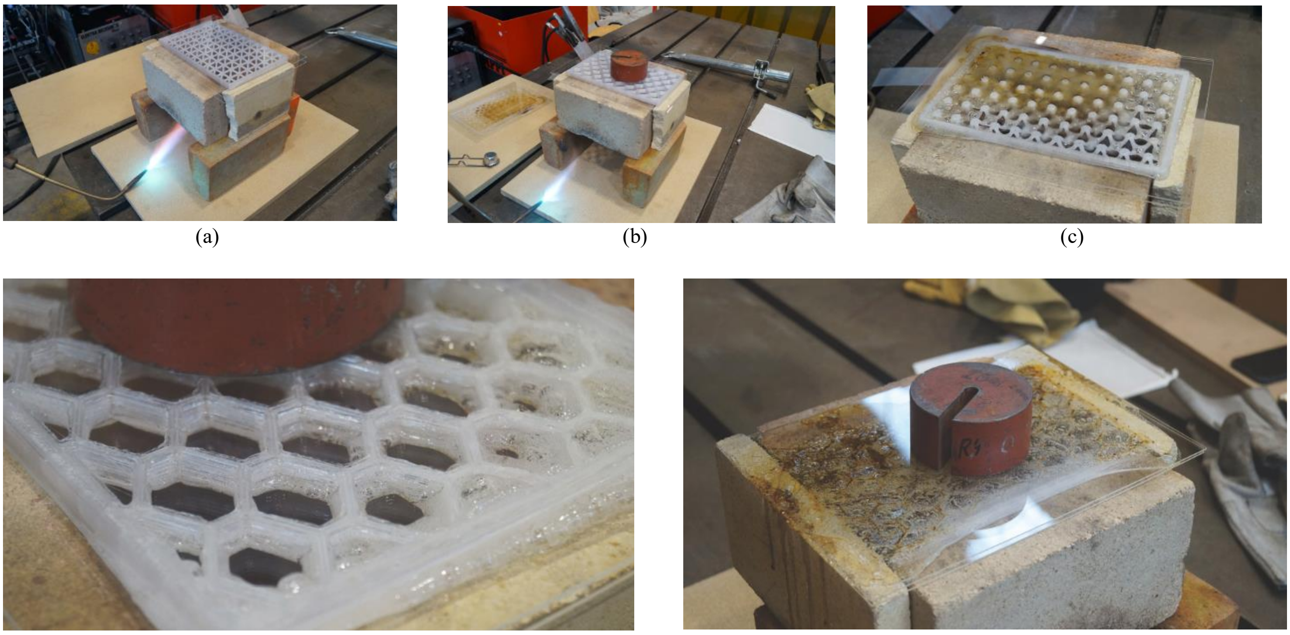

(a) (b) (c) (d) (e)

Fig. 16a) Heating up the setup and composite panel without a load, b) Heating up the setup and composite panel with a load, c) Melting of the recycled PET core, d) Melting of the core layer by layer, e) Core fully melted and partly burned.

## 6. Conclusion

The main goal of this study was to explore the durability of a lightweight and rigid thin glass composite panel. This study showed that the combination of recycled PET and thin glass can create a stiff and lightweight sandwich panel with a weight reduction of 71.9 % compared to regular glass panels.
The durability aspects (UV radiation, elevated temperatures during summer conditions and fire exposure) impact the composite panel, leading to a reduction in stiffness and strength. Firstly, UV radiation causes a color change (core becomes yellowish). This is due to photo-degradation and which induces the original color/translucency to fade away and become more brittle. Secondly, the strength of the core element decreases due to UV exposure.
At elevated temperatures, the composite panel outer surface can reach up to a temperature of 80 $^{o}$C. At this temperature it is shown that the composite still take forces up, but the panel behaves less rigid. When the temperature decreases again down to room temperature , the core element becomes stiff again.
During a fire scenario, the recycled PET core element will melt completely due also to the relatively low thickness, which allows for a relatively high thermal transmittance. The composite panel will lose its stiffness. However, the glass panels will stay intact and would not fail.

**Acknowledgements**

The authors would like to the thank AGC for providing the thin glass for this study. Furthermore, the authors are grateful for the support of the material science lab at 3ME TU Delft in facilitating the structural tests, and LAMA the TOI's Lab for Additive Manufacturing in Architecture.

## References

AGC. *Falcon Glass.* Retrieved from AGC Glass (2017): https://www.yourglass.com/yourglass3/content/catalog/applications/industrial/Special_compositions/brochures/FALCON/display.pdf

Al-Sabagh, A. M., Yehia, F. Z., Eshaq, G., Rabie, A. M., ElMetwally, A. E.: Greener routes for recycling of polyethylene terephthalate. Egyptian Journal of Petroleum, 25(1), 53–64 (2016)

Aluminosilicate glass. Retrieved May 20 (2018), from Continental Trade: https://www.continentaltrade. com.pl

Apaza, E.: Sandwich panels. Retrieved June 5 (2018), from Slideshare: https://www.slideshare. net/eusebioapaza/sandwich-panels-16529813

Ashby, A. M. F.: The Properties of Foams and Lattices THE, 364(1838), 15–30 (2006)

Awaja, F., Pavel, D.: Recycling of PET. Eur. Polym. J. 41(7), 1453–1477 (2005). https://doi.org/10.1016/j.eurpolymj.2005.02.005

Baechler, C., DeVuono, M., Pearce, J. M.: Distributed recycling of waste polymer into RepRap feedstock. Rapid Prototyping J. 19(2), 118–125 (2013)

CESEduPack. Alumino silicate - 1720. Granta Design Limited. Retrieved May 24 (2018)

Conner, B. P., Manogharan, G. P., Martof, A. N., Rodomsky, L. M., Rodomsky, C. M., Jordan, D. C., Limperos, J. W.: Making sense of 3-D printing: Creating a map of additive manufacturing products and services. Addit. Manuf. 1, 64–76 (2014)

Corning. Science of Glass: How It Works - Fusion Process. Retrieved May 8 (2018), from Corning: https:// www.corning.com/worldwide/en/innovation/the-glass-age/science-of-glass/how-it-works-cornings-fusionprocess.html

Delgado, D., Clayton, P., Brien, W. J. O., Seepersad, C., Juenger, M., Ferron, R., Salamone, S.: Applications of additive manufacturing in the construction industry – A forward-looking review. Autom. Constr. 89, 110–119 (August 2017)

EllenMacArthurFoundation. The New Plastics Economy: Rethinking the future of plastics. World Econimic Forum and Ellen MacArthur Foundation (2014). Retrieved from https://www.ellenmacarthurfoundation.org/assets/ downloads/EllenMacArthurFoundation_TheNewPlasticsEconomy_Pages.pdf

Haldimann, M., Luible, A., Overend, M.: Structural use of glass. Zürich: International Association for Bridge and Structural Engineering (2008)

Hundevad, J.: Super lightweight glass structures – a study. GlassCon Global - Innovation in Glass Technology, 324–337 (2014)

Kreiger, M. A., Mulder, M. L., Glover, A. G., Pearce, J. M.: Life cycle analysis of distributed recycling of post-consumer high density polyethylene for 3-D printing filament. J. Cleaner Prod. 70, 90–96 (2014)

Lim, S., Buswell, R. A., Le, T. T., Austin, S. A., Gibb, A. G. F., Thorpe, T.: Developments in construction-scale additive manufacturing processes. Autom. Constr. 21(1), 262-268 (2012)

Louter, C., Akilo, M., Miri, B., Neeskens, T., Ribeiro Silveira, R., Topcu, Ö., . . . O'Callaghan, J.: Adaptive and composite thin glass concepts for architectural applications. HERON: Structural glass, 199-218 (2018)

López-Fonseca, R., Duque-Ingunza, I., de Rivas, B., Flores-Giraldo, L., & Gutiérrez-Ortiz, J. I.: Kinetics of catalytic glycolysis of PET wastes with sodium carbonate. Chem. Eng. J. 168(1), 312–320 (2011)

Neeskens, T.: Thin glass composites: based on a structural efficiency increasing design strategy. Delft: TU Delft (2018). Retrieved from: https://repository.tudelft.nl/islandora/search/tim%20neeskens?collection=education

Park, S., Kim, S.: Poly (ethylene terephthalate) recycling for high value added textiles. Fashion Text. 1, 1–17 (2014)

Pilkington. Extremely thin float glass: Pilkington Microfloat Pilkington Microwhite. Ohio: Pilkington North America (2014). Retrieved from http://www.pilkington.com

Pingle, S. M., Fleck, N. A., Deshpande, V. S., Wadley, H. N. G.: Collapse mechanism maps for a hollow pyramidal lattice. Proceedings of the Royal Society A: Mathematical, Physical and Engineering Sciences, 467(2128), 985-1011 (2011)

PTI. Research study: PET bottles exposed to UV light. Retrieved June 6, 2018, from PTI: https://www.plastictechnologies.com/news/2015/07/research-study-pet-bottles-exposed-to-uv-light.aspx

Silveira, R.: Flexible Transparancy: A study on thin glass adaptive façade panels. Delft: Delft University of Technology (2016). Retrieved from: https://repository.tudelft.nl/islandora/object/uuid%3Afd32f4fc-6dab-4468-83f2-53abcc12e715?collection=education

Siegele, C.: Thin Glass Revolutionising the Performance Spectrum of Glass and Glass Panes. Retrieved May 8, 2018, from Intelligent Glass Solutions: http://igsmag.com/editors-picks/thin-glass-revolutionis-ing-performance-spectrum-glass-glass-panes/

Vitalis, D., Veer, F., Oikonomopoulou, F.: Design and Experimental Testing of All Glass Sandwich Panels: An Experimental and Numerical Study for the Glass Floors of the Acropolis Museum. In Challenging Glass Conference Proceedings (Vol. 6, pp. 251-270) (2018, May).

Wadley, H. N. G.: Multifunctional periodic cellular metals, 31–68 (December 2005)

Weller, B., Unnewehr, S., Tasche, S., Härth, K. Glass in building: principles, applications, examples. Walter de Gruyter (2009)

*Challenging Glass 7*
*Conference on Architectural and Structural Applications of Glass*
*Belis, Bos & Louter (Eds.), Ghent University, September 2020.*
*ISBN 978-94-6366-296-3, www.challengingglass.com*

PLATINUM SPONSORS

GOLD SPONSORS

SILVER SPONSORS

ORGANISING PARTNERS